Curtin
UNIVERSITY OF TECHNOLOGY

Centre for Marine Science and Technology

HYDRODYNAMIC FORCES ON UNDERWATER CABLES

By:
Edward Dawson

Prepared for:
Dr Kim Klaka

PROJECT CMST #
REPORT C2005-06

14 January 2005

ABSTRACT

This report reviews several existing methods used to derive hydrodynamic force equations and coefficients and the simulation models in which they are used to predict the position and motions of underwater cables. The report focus on the hydrodynamic forces acting on submerged cylindrical tow cables in relative flow at small angles of attack. Relevant findings presented in the thesis *An Experimental Study of Hydrodynamic Forces on Cylinders and Cables in Near Axial Flow* are included, along with brief theoretical explanations and evaluations of simulation models.

TABLE OF CONTENTS

1 Introduction 4
2 Cross-Flow Theory 4
3 Thesis Examining Hydrodynamic Forces 5
3.1 The Approach Used to Model the Hydrodynamic Forces 5
3.2 Possible Flow Regimes 6
3.3 Experimental Analysis 6
3.4 Experimental Results Used to Produce a Linear Model 6
3.5 Summary of Results 7
3.5.1 Results of the Physical Experiments 7
3.6 Equations of Motion 15
4 Vortex Shedding Phenomena 16
5 Mathematical Models and Simulations 16
6 Conclusion 17
References 18

1 INTRODUCTION

The use of underwater remotely operated vehicles (ROV) and towed sensory equipment such as acoustic transducers and SONAR arrays, is extensive in both commercial and government sub-sea operations. The cable, umbilical or tether is a fundamental part of the operation of such equipment. In order to optimize aspects of operation such as safety and efficiency, accurate information indicating the instantaneous position and attitude of the cable and instrument during operation needs to be available to the operator. Various numerical models, which can be solved using computer software, have been generated to predict the cable's motions and position. An ideal model would, among other traits, display the ability to return an accurate prediction for the range of operational circumstances in an elapsed time significantly less than that of real time. It has been identified that the choice of coefficients used to determine the external hydrodynamic forces is one of the main sources of error within the simulation's design, particularly for small angles of attack Gourlay & Duncan (2004).

2 CROSS-FLOW THEORY

During the operation of tethered submerged equipment it is common for the cable to be subjected to a range of incidence angles relative to the direction of the oncoming flow. These angles may extend from zero degrees, where the cable is axially aligned with the flow, through to 90 degrees where the cable is normal to the flow. When analyzing the cable it is common to consider it to be a cylindrical object. As the angle of attack experienced by the cylinder varies so does the hydrodynamic force acting upon it. An important phenomenon known as the Cross-Flow principle, presented by Hoerner (1965) and Sumer & Fredsøe (1999), suggests that for inclined cylinders with an angle of attack between 45 and 90 degrees, the fluid passing around the cylinder deflects such that it encounters the cylinder at an angle of 90 degrees, relative to the cylinder's axis. This implies that the relative cylinder-fluid velocity will be that of the upstream rather than a resolved component. The behavior of the cross-flow phenomenon varies as the flow conditions vary for example separated or attached flow. This is important when generating the hydrodynamic force equations and their coefficients.

While extensive experimental research has been performed to define the hydrodynamic forces acting on the cylinder for normal flow, only limited work has been done to account for the circumstances where the cross-flow principle does not apply. It is in the range of low angle of attack, between zero and approximately 45 degrees, which cables used for towing submerged equipment operate. A recent study conducted at the Norwegian University of Science and Technology by Ersdal (2004) presents both experimental data and a simulation model for cables in near axial flow.

3 THESIS EXAMINING HYDRODYNAMIC FORCES

Ersdal's thesis examines the hydrodynamic forces acting on a submerged cylinder that is subject to relative motion at small angles of attack. He uses empirical data to discuss the validity of current hydrodynamic theories, in particular the cross flow theory and the 2D+t principle. A range of experimental force data is presented for three tow configurations: rigid cylinder at stationary angles, oscillating rigid cylinder, and oscillating flexible cylinder. Ersdal uses this data, along with previously established modelling techniques, to derive a Time Domain Finite Element model involving second order elements simulating the cylinder's motion. Due to the lack of existing experimental data, Ersdal uses extensive error and uncertainty analysis to verify the quality of the data presented. The error of the formulated hydrodynamic model is estimated at 10 percent.

3.1 The Approach Used to Model the Hydrodynamic Forces

The approach Ersdal uses to model the hydrodynamic forces involves decomposing the net hydrodynamic force into forces acting due to potential flow effects and forces acting due to viscous flow effects; examples of each are given in Ersdal (2004) page 4. The potential flow forces are modelled using the slender body approximation, outlined in Ersdal (2004) page 8. The viscous forces are modelled using a typical lift coefficient equation.

3.2 Possible Flow Regimes

Through the analysis of the normal forces acting on a rigid cylinder towed at a constant angle of attack, for angles between zero and twenty degrees, two possible flow regimes have been identified. Ersdal suggests that the propagation of symmetric or asymmetric vortices is an important occurrence influencing the magnitude of the normal hydrodynamic forces. The results indicate that when symmetric vortices are initiated, the characteristics of the normal force relate closely to those recorded in previous studies. When asymmetric vortices are initiated, the normal force varies linearly with the angle of attack for small angles. The cross-flow theory is found to be valid for greater angles of attack subject to laminar flow; a change to turbulent flow affects the equation's coefficient.

3.3 Experimental Analysis

Ersdal uses the experimental analysis of the rigid cylinder subjected to forced oscillations to derive possible force models. The dependence of the hydrodynamic force on the Keulegan-Carpenter number is examined and found to diminish as the axial velocity of the cylinder increases and have little importance for angles of attack less than 15 degrees. Where the angle of attack is less than 0.5 degrees, the separation of the flow is found to be limited and it is suggested that the linear term is replaced by the friction coefficient. Other findings from the rigid cylinder experiments suggest that for circumstances where the cylinder is subject to the cross-flow effect the drag coefficient is dependent on the Reynolds number of the longitudinal flow.

3.4 Experimental Results Used to Produce a Linear Model

The experimental results obtained for the oscillating flexible cylinder, in particular the response due to harmonic oscillation, are analysed and utilized to produce a linear model of the transverse motion of a cylinder; the Paidoussis equation (the main assumptions relating to this equation are outlined on page 85). The Paidoussis equation is further developed to include non-linear hydrodynamic forces. Using the data recorded for the rigid cylinder, the accuracy of this equation is increased. While the accurate estimation of the hydrodynamic forces implies an accurate model, a single model accurate for all oscillatory frequencies has not been formulated.

Ersdal presents a completed equation of motion, including internal and external forces, in chapter 6.

The Finite Element Method developed by Ersdal provides a time domain simulation of the transverse motion of a towed flexible cylinder experiencing small oscillations and near neutral buoyancy. The main influencing parameters on the model are the cylinder (cable) diameter and the coefficients used to model the hydrodynamic forces including the longitudinal friction coefficient.

Ersdal suggests that further research using computational fluid flow visualisation and experimental towing and testing is required to provide a concise explanation of the possible three-dimensional asymmetric vortex-shedding phenomena.

3.5 Summary of Results

3.5.1 Results of the Physical Experiments

Fixed and Oscillating Rigid Cylinder

The results presented in tables B.1 – B.4 indicate the following force and moment coefficients for a rigid cylinder being towed at specific velocities:

C_{n2} is the normal force coefficient when rotating in yaw for forces acting in the y direction and is described by:

$$C_{n2}(\alpha) = (F_y^a + F_y^f) / (\tfrac{1}{2}\rho U^2 \, dL)$$

C_{n3} is the bi-normal force coefficient when rotating in yaw for forces acting in the z direction and is described by:

$$C_{n3}(\alpha) = (F_z^a + F_z^f) / (\tfrac{1}{2}\rho U^2 \, dL)$$

C_{n5} is the bi-normal moment coefficient when rotating in yaw. The moment is taken at approximately L/2 and is described by:

$$C_{n5}(\alpha) = (-F_z^a + F_z^f) / (\tfrac{1}{2}\rho U^2 \, dL)$$

C_{n6} is the normal moment coefficient when rotating in yaw. The moment is taken at approximately L/2 and is described by:

$$C_{n6}(\alpha) = (-F_y^a + F_y^f) / (\tfrac{1}{2}\rho U^2 \, dL)$$

Where:

α is the angle of attack measured in degrees. It is the angle between the tangential direction of the cylinder and the incoming flow.

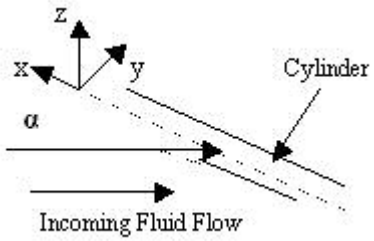

U is the tow speed measured in m/s.

F is the force vector measured in Newtons.

The superscripts '*f*' and '*a*' denote the force measured by the sensors positioned forward and aft of the test section respectively.

The subscripts 'y' and 'z' indicate the direction of the normal and bi-normal forces measured relative to the coordinate system.

The force normal to the cylinder's axis and in the plane of the oncoming flow is defined as the normal force, while the force normal to this plane is known as the bi-normal force. The rotation of the cylinder about the y-axis, as defined in figure 3.0, is defined as pitch and rotations about the z-axis is defined as yaw. In the cases where the model was rotated in pitch, the z-axis is the normal and the y-axis is the bi-normal. Similarly, where the model is rotated in yaw, the y-axis becomes the normal and the z-axis becomes the bi-normal.

The error (e) represents the 95% confidence interval.

The coordinate system used by Ersdal to define the test model is shown below:

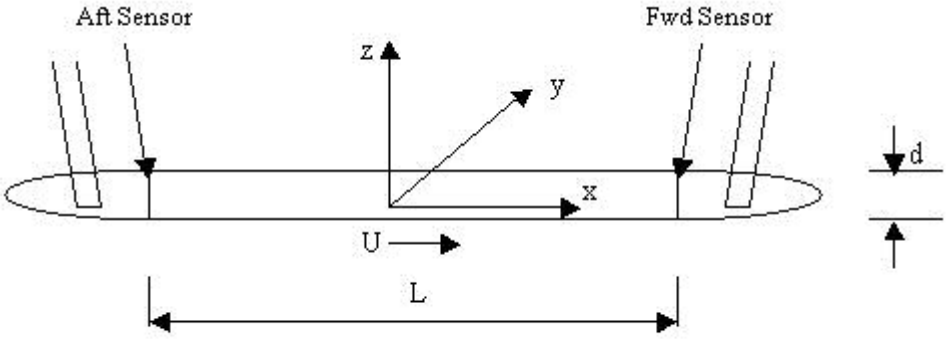

Figure 3.0: *Test model coordinate system.*

The setup and procedure for the rigid, rigid oscillating and flexible oscillating experiments are presented in chapters 3, 4 and 5 respectively.

Table 3.1: Parameters of the test section

Length	L	2.03 m
Diameter	d	0.051 m
Dry Weight	m	1.875 kg
Water density	ρ	998.5 kg/m^3
Dynamic viscosity	υ	1.05x10^{-6} m^2/s
Length to diameter ratio	L/d	39.2
Structural mass to Added mass ratio	$4m_s/\pi d^2$	0.46
Roughness	k/d	29.5x10^{-6}

Table B.1: Force coefficients for rigid cylinder and constant yaw angle, U = 1.0 m/s

α	C_{n2}	e_2	C_{n3}	e_3	C_{n5}	e_5	C_{n6}	e_6
-2	-0.0016	0.001	-0.0023	0.0027	0.00072	0.0036	0.00011	0.00087
-1	-0.00055	0.00026	0.00044	0.0021	0.0018	0.0037	-9.90E-05	0.00024
0	0	0	0.0019	0.0022	0.0016	0.0038	0	7.90E-05
1	0.0023	0.00023	0.00087	0.0024	0.0015	0.004	7.00E-05	0.0006
2	0.0034	0.00042	-0.0017	0.0032	0.0013	0.0031	-0.00015	0.00029
3	0.0046	0.00053	-0.0037	0.0033	0.0012	0.0024	-8.60E-05	0.00032
4	0.0058	0.00096	-0.0053	0.0036	0.0013	0.0025	-0.00028	0.00073
6	0.0097	0.0018	-0.0074	0.0028	0.00083	0.0064	0.00019	0.00075
8	0.016	0.0015	-0.0083	0.0029	0.00065	0.008	0.00086	0.00077
10	0.03	0.004	-0.0074	0.0035	-0.00011	0.011	0.0021	0.00095
12	0.054	0.005	0.0018	0.0027	0.0021	0.015	0.0035	0.0023
16	0.097	0.0018	0.0025	0.0024	0.0019	0.0081	0.0065	0.0032
20	0.17	0.0049	0.018	0.0021	0.0042	0.029	0.0085	0.0074
25	0.25	0.0067	0.013	0.0073	0.0069	0.025	0.011	0.012
30	0.32	0.0053	0.016	0.014	0.0067	0.037	0.012	0.017

Table B.2: Force coefficients for rigid cylinder and constant yaw angle, U = 1.5 m/s

α	C_{n2}	e_2	C_{n3}	e_3	C_{n5}	e_5	C_{n6}	e_6
-2	-0.0024	0.00054	-0.0036	0.0022	0.00056	0.0029	3.40E-05	0.0011
-1	-0.00075	0.00021	0.00057	0.0021	0.00081	0.0033	-6.20E-05	0.00039
0	0	0	0.0019	0.0022	0.00097	0.0034	0	3.00E-05
1	0.0021	0.00027	0.00094	0.0025	0.00088	0.0032	-1.30E-04	0.00054
2	0.0033	0.00061	-0.0017	0.0032	0.00072	0.0028	-0.00024	0.00028
3	0.0044	0.00045	-0.0041	0.0035	0.00079	0.0021	-1.30E-04	0.00022
4	0.0058	0.00069	-0.0057	0.0034	0.00087	0.0027	-0.00022	0.00064
6	0.0098	0.0013	-0.0076	0.0028	0.0012	0.0076	0.00049	0.00053
8	0.016	0.002	-0.0089	0.0023	0.00036	0.0092	0.0007	0.00051
10	0.024	0.0022	-0.0083	0.0024	0.0015	0.013	0.0013	0.00088
12	0.034	0.0039	-0.0097	0.0022	0.0015	0.014	0.002	0.0016
16	0.091	0.0041	0.00053	0.0022	0.0018	0.011	0.0062	0.0057
20	0.16	0.0035	0.019	0.0051	0.0011	0.03	0.0099	0.011
25	0.25	0.0048	0.0089	0.0023	-0.0006	0.028	0.013	0.0095
30	0.31	0.0093	0.011	0.0036	0.0022	0.055	0.015	0.011

Table B.3: Force coefficients for rigid cylinder and constant yaw angle, U = 2.0 m/s

α	C_{n2}	e_2	C_{n3}	e_3	C_{n5}	e_5	C_{n6}	e_6
-2	-0.0025	0.00054	-0.0044	0.0024	2.30E-05	0.0025	-8.10E-06	0.0011
-1	-0.0011	0.00039	-0.00012	0.0021	0.00033	0.0029	-1.50E-04	0.00044
0	0	0	0.0017	0.0021	0.00058	0.0029	0	1.50E-05
1	0.002	0.00033	0.00079	0.0024	0.0006	0.0028	-8.00E-05	0.00047
2	0.003	0.00048	-0.0021	0.0031	0.00058	0.0024	0.00015	0.00064
3	0.0043	0.00043	-0.0044	0.0037	0.00072	0.002	-2.10E-04	0.00041
4	0.0055	0.00067	-0.0061	0.0042	0.001	0.003	-0.00031	0.00079
6	0.0092	0.0013	-0.008	0.0033	0.0016	0.0081	0.00034	0.00071
8	0.015	0.0018	-0.0093	0.0026	0.0017	0.0095	0.00058	0.00043
10	0.024	0.0022	-0.009	0.0032	0.0025	0.013	0.0012	0.001
12	0.033	0.0033	-0.0095	0.0025	0.0026	0.014	0.002	0.0019
16	0.059	0.0093	-0.0069	0.0039	0.00027	0.022	0.0056	0.0083
20	0.16	0.0025	0.011	0.0077	-0.00054	0.039	0.0099	0.0086
25	0.24	0.0045	0.00096	0.007	-0.0011	0.038	0.013	0.0042

Table B.4: Force coefficients for rigid cylinder and constant yaw angle, U = 2.5 m/s

α	C_{n2}	e_2	C_{n3}	e_3	C_{n5}	e_5	C_{n6}	e_6
-2	-0.0023	0.00041	-0.0042	0.0025	-0.00013	0.0022	-1.40E+05	0.00094
-1	-0.00098	0.0004	7.00E-05	0.0022	0.00023	0.0024	-1.10E-04	0.00038
0	0	0	0.0019	0.0021	0.00041	0.0024	0	8.20E-06
1	0.0019	0.00026	0.00081	0.0022	0.00043	0.0023	-5.40E-05	0.0005
2	0.0031	0.00039	-0.002	0.0031	0.00036	0.0021	-0.00013	0.00024
3	0.0042	0.00046	-0.0046	0.0039	0.00058	0.0022	-2.40E-04	0.00042
4	0.0052	0.00054	-0.0062	0.0044	0.00079	0.0034	-0.00024	0.00068
6	0.009	0.0011	-0.0089	0.0028	0.0011	0.0089	0.00037	0.00068
8	0.015	0.0019	-0.0097	0.003	0.0018	0.01	0.00048	0.00052
10	0.023	0.0023	-0.0092	0.0032	0.0024	0.014	0.0013	0.00091
12	0.033	0.0036	-0.01	0.0028	0.0026	0.014	0.002	0.0016
16	0.055	0.0031	-0.0092	0.002	0.00058	0.023	0.0039	0.0052
20	0.14	0.017	0.0088	0.015	0.0028	0.036	0.0048	0.0086
25	0.22	0.0058	-0.0062	0.016	-0.0015	0.042	0.012	0.0026

Table B.5: Force coefficients for rigid cylinder and constant pitch angle, U = 1.0 m/s

α	C_{n2}	e_c [%]	C_{n3}	e_c [%]	C_{n5}	e_c [%]	C_{n6}	e_c [%]
0	-0.000653	-72.5	-0.000292	-175	-0.000326	26.2	-0.000162	-131
1	-0.000271	-618	-0.000193	-72.6	-0.000491	16.3	-1.94E-04	13.7
2	0.000912	149	0.000445	92.6	-6.23E-05	-322	-6.97E-05	-272
3	0.00144	5.81	0.00088	39.2	-2.04E-05	8.97	9.06E-05	-3.31
4	0.00266	39.7	0.0013	16	0.000111	-290	0.000272	-12.7
6	0.00627	7.28	0.00201	31	5.09E-06	5.18	0.00127	10.8
8	0.0113	3.09	0.00268	51.1	-0.000199	36.6	0.00161	15.2
10	0.0195	9.57	0.00284	43	-0.00091	54.2	0.00196	28.9
12	0.0314	5.2	0.00216	118	-0.00085	-9.15	0.00215	44.9

Table B.6: Force coefficients for rigid cylinder and constant pitch angle, U = 1.5 m/s

α	C_{n2}	e_c [%]	C_{n3}	e_c [%]	C_{n5}	e_c [%]	C_{n6}	e_c [%]
0	-0.000416	-29.8	9.93E-05	287	-0.000208	-22.6	-6.06E-05	-7.43E+01
1	5.81E-05	1.16E+03	-0.000113	-186	-0.000297	83.1	-7.56E-05	-13.6
2	0.000777	109	4.36E-05	706	-0.000274	115	-1.54E-05	594
3	0.0017	51.2	0.000187	372	-0.000205	170	5.64E-05	-147
4	0.00274	10.9	0.000465	179	-9.77E-05	72.9	0.000178	83.5
6	0.00608	9.31	0.000721	170	-0.000101	62.3	0.00077	58.2
8	0.0104	13.9	0.00161	136	-0.000147	143	0.00101	66.6
10	0.0165	5.21	0.00218	155	-0.00041	-13.6	0.00144	90.3
12	0.023	5.7	0.000977	472	-0.000677	-14.4	0.0017	123

The following results indicate the peak-to-peak force amplitude for a combination of circular frequencies (ω) and tow velocities. To avoid large deflections in the cylinder supports the oscillations were performed in the vertical z-direction. The force values shown are the result of subtracting the dry mass inertia force from the measured force. Ersdal suggests that the results represent the hydrodynamic force only. In this case the z-direction describes the normal forces and the y-direction describes the bi-normal forces. The error *e* represents the 95% confidence interval.

Table B.7: Peak-to-peak force amplitude for oscillating rigid cylinder.

Tow Speed [m/s]	ω_0 [rad/s]	F_y [N]	e	F_z [N]	e
0.0	0.15	0.44	0.32	1.00	0.13
	0.20	1.56	0.92	2.03	0.33
	0.25	2.84	1.45	3.38	0.82
	0.30	3.27	1.54	4.56	0.71
	0.35	5.51	2.92	6.20	0.79
	0.40	3.16	3.39	6.87	1.03
0.2	0.05	0.10	0.08	0.36	0.07
	0.10	0.14	0.17	0.62	0.08
	0.14	0.26	0.17	0.95	0.10
	0.18	0.59	0.34	1.41	0.12
	0.22	1.30	0.32	2.02	0.15
	0.26	1.92	0.84	2.76	0.29
	0.29	1.36	1.03	3.52	0.28
	0.32	1.12	0.49	4.27	0.32
	0.36	2.09	1.32	5.06	0.39
0.4	0.05	0.15	0.12	0.39	0.08
	0.10	0.14	0.09	0.66	0.09
	0.15	0.34	0.23	0.89	0.09
	0.19	0.39	0.17	1.45	0.12
	0.24	1.09	0.29	2.15	0.15
	0.28	1.86	0.64	2.96	0.16
	0.32	1.95	0.96	4.00	0.27
	0.36	1.92	0.79	5.04	0.29
0.6	0.05	0.21	0.10	0.72	1.07
	0.10	0.47	0.33	0.86	0.45
	0.15	0.30	0.18	0.98	0.34
	0.20	0.52	0.21	1.27	0.30
	0.24	1.12	0.27	1.87	0.16
	0.29	1.77	0.32	2.78	0.25
	0.33	2.27	0.43	3.87	0.24
	0.37	2.33	0.46	5.06	0.35
1.0	0.05	0.40	0.16	0.73	1.12
	0.10	0.61	0.93	0.77	0.30
	0.15	0.55	0.41	1.04	0.34
	0.20	0.67	0.43	1.28	0.19
	0.25	0.68	0.40	1.63	0.22
	0.29	0.77	0.65	1.92	0.21
	0.34	0.92	0.47	2.40	0.20
	0.39	1.22	0.42	3.21	0.22

Oscillating Flexible Cylinders

The results in Table B.8 indicate the peak-to-peak amplitude of motion (A_{pp}) for a combination of circular frequencies (ω) and tow velocities. To avoid large deflections in the cylinder supports the oscillations were performed in the vertical z-direction. In this case the z-direction describes the normal forces and the y-direction describes the bi-normal forces. The error (*e*) represents the 95% confidence interval.

Table 5.1: Parameters for the cable used in experiments.

Tow speed:	U =	0.5 -2.5 m/s
Diameter:	d =	0.011 m
Length to diameter ratio:	L/d =	1180
Reynolds numbers	Re_L	0.65-3.25 $x10^7$
Distributed structural mass:	q =	97.5$x10^{-3}$ kg/m
Aft tension	T_0 =	19.6 N
Aft spring stiffness	k_p =	48.2 N/m
Period of oscillation	T_p =	0.3-30 s
Amplitude of oscillation:	A_0 =	0.05 m

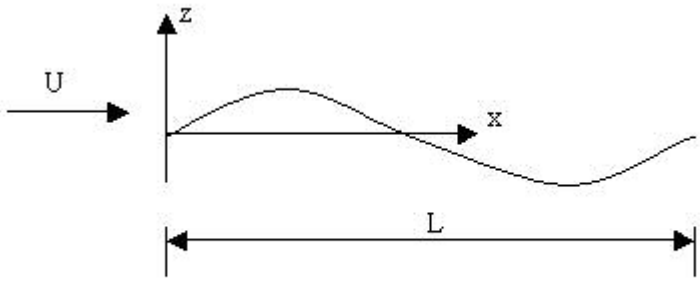

Figure 5.2: *Reference system for the flexible cylinder.*

Table B.8: Peak-to-peak amplitude for oscillating flexible cylinder at x/L = 0.77.
Force amplitude at x/L = 0 is 0.01 m

		y-direction		z-direction	
Tow Speed U [m/s]	ω [rad/s]	$A_{pp\,y}$ [m]	e [m]	$A_{pp\,z}$ [m]	e [m]
0.0	2.4525	0.0075	0.0042	0.0237	0.0036
	6.2722	0.0036	0.0030	0.0082	0.0018
	9.5985	0.0038	0.0032	0.0029	0.0019
0.5	0.2109	0.0028	0.0011	0.0238	0.0006
	0.3187	0.0028	0.0013	0.0237	0.0015
	0.5841	0.0025	0.0014	0.0263	0.0006
	0.8402	0.0025	0.0013	0.0284	0.0006
	1.2122	0.0032	0.0017	0.0329	0.0006
	2.4505	0.0053	0.0040	0.0304	0.0033
	6.2768	0.0029	0.0024	0.0101	0.0020
	9.6008	0.0020	0.0021	0.0022	0.0013
	18.4638	0.0039	0.0035	0.0025	0.0019
1.5	0.2094	0.0040	0.0011	0.0249	0.0006
	0.2668	0.0060	0.0011	0.0278	0.0006
	0.5858	0.0051	0.0017	0.0312	0.0012
	0.8431	0.0042	0.0012	0.0324	0.0036
	1.2157	0.0052	0.0019	0.0352	0.0018
	2.4505	0.0044	0.0018	0.0290	0.0014
	6.2768	0.0016	0.0017	0.0097	0.0014
	9.6040	0.0010	0.0015	0.0029	0.0012
	18.4824	0.0028	0.0026	0.0017	0.0015
2.5	0.2094	0.0077	0.0011	0.0327	0.0006
	0.3142	0.0100	0.0011	0.0322	0.0006
	0.5843	0.0170	0.0011	0.0335	0.0006
	0.8422	0.0161	0.0022	0.0383	0.0014
	1.2215	0.0056	0.0024	0.0381	0.0026
	2.4510	0.0046	0.0027	0.0286	0.0013
	6.2808	0.0022	0.0021	0.0069	0.0037
	9.6193	0.0027	0.0023	0.0037	0.0013
	18.5405	0.0035	0.0022	0.0027	0.0021

3.6 Equations of Motion

The set of two linear equations of motion derived by Ersdal, originally developed by Paidoussis, are presented in chapter 6. The main assumptions are that the transverse motions and velocities are small compared to the axial velocity and dimensions of the cylinder, and that the internal forces related to the bending stiffness and material damping are neglected. The equations account for the internal cable tension, its weight, buoyancy and hydrodynamic forces in both the tangential and axial planes.

The net hydrodynamic force acting on the cylinder is resolved into two components: a normal (F_n) and a tangential (F_t). The normal component is equal to the sum of the potential flow term (F_{np}) and a term due to the viscous effects (F_{nv}).

The potential force term is given by:

$$F_{np} = -a(\partial^2 z/\partial t^2) - a(\partial/\partial x)\{2U(\partial z/\partial t) + U^2(\partial z/\partial x)\}$$

The viscous force term is given by:

$$F_{nv} = C_n \tfrac{1}{2}\rho U\{(\partial z/\partial t) + U(\partial z/\partial x)\}d$$

The set of linear equations are:

$$\boldsymbol{q\,(\partial^2 x/\partial t^2) = (\partial/\partial x)T(x) + f_t - B(\partial z/\partial x)}$$

$$\boldsymbol{m\,(\partial^2 z/\partial t^2) = (\partial/\partial x)\{Q(x)(\partial z/\partial x) - a_1(\partial z/\partial t)\} + f_t\,(\partial z/\partial x) - f_{n1}\{(1/U)(\partial z/\partial t) + (\partial z/\partial x)\} - w}$$

Where:

$m = q + a$	*Dry mass + added mass (per unit length)*
$Q(x) = T(x) - aU^2 + Bh$	*Tension – component of the external normal force due to potential flow + product of buoyancy and depth*
$a_1 = 2aU$	*Component of external normal force due to potential flow*
$f_t = \pi C_F \tfrac{1}{2}\rho d U^2$	*Tangential force*
$f_{n1} = C_{n1} \tfrac{1}{2}\rho d U^2$	*Normal force*
$w = W - B$	*Weight – Buoyancy*

'a' is the two dimensional added mass which is considered to be constant along the length of the cable except at the boundaries.

4 VORTEX SHEDDING PHENOMENA

The vortex shedding phenomena is identified by Ersdal (2004) as an important contributing factor to the magnitude of the hydrodynamic force acting on a tow cable. A system to categorise the flow separation and vortex shedding is presented by Cummings et al. (2003) along with a review of current predictive capabilities and a solution based on hybrid turbulence models. Cummings et al. (2003) examines the use of Reynolds-averaged Navier-Stokes (RANS), large eddy simulation (LES) and direct numerical simulation (DNS) to provide numerical predictions of turbulent flows around aircraft fuselage. It is assumed that an accurate numerical model, defining the flow behaviour around slender bodied cylinders, will further increase the accuracy of simulations, such as Ersdal's (2004), across a wider range of operating angles of attack.

5 MATHEMATICAL MODELS AND SIMULATIONS

As there is a continuing need for more accurate and effective mathematical models and simulations, describing the position and motions of underwater equipment and their associated tethers, an increasing number of models are being derived and their associated hydrodynamic characteristics researched. Several of the simulations and their modelling techniques have been reviewed and a brief evaluation of two of the more credible methods is given in this section.

Cable and Vehicle Model

The model and simulation presented by Perrault et al. (1997) uses a lumped mass method to describe the motions of the cable connecting an undersea vehicle to a surface-operating platform. A separate model was created for both the cable and the undersea vehicle and then coupled to provide a single simulation. The method used to validate the cable model was compared to the simulations and experimental data presented by Patel & Vaz (1995). Perrault et al. suggests that the results of their simulation are a close match to those of Patel & Vaz. The hydrodynamic force equations used by Perrault et al. include a loading function and a function defining the sign of the normal and tangential drag.

Three Dimensional Model of an Underwater Cable

A three dimensional computer code using a finite difference approximation to model the dynamics of an underwater cable is presented by Ablow & Schechter (1983). The code generates a three dimensional representation of the cable and indicates the tensions along the cable length and the velocity at each of its node points. Several testing operations are used to verify the accuracy of the code, among which is simulation comparisons with data provided from full-scale manoeuvres. The results of the simulation are considered by Ablow & Schechter to compare favourably with the experimental data; some aspects differ by less than 2%. The simulation is found to run at a less than real time speed.

6 CONCLUSION

As commercial and government sub-sea and offshore operations require increasingly effective and operable underwater ROV and towed sensory equipment there is a demand to produce accurate and efficient simulation software. A number of mathematical models and simulations have been produced using experimental research and existing modeling methods. While some simulations appear to produce relatively accurate predictions, the choice of coefficients used to model the external hydrodynamic forces and the impact of cylinder-flow field behavior is a significant limiting factor, especially for instances of small angles of attack.

REFERENCES

Ablow, C.M. & Schechter, S. 1983. *Numerical Simulation of Undersea Cable Dynamics*. Ocean Engineering 10(3), 443-457.

Cummings, R.M., Forsythe, J.R., Morton, S.A.,& Squires, K.D. 2003. *Computational Challenges in High Angle of Attack Flow Prediction*. Progress in Aerospace Sciences, 39 (2003), 369-384.

Ersdal, S. 2004. *An Experimental Study of Hydrodynamic Forces on Cylinders and Cables in Near Axial Flow*. Department of Marine Technology, NTNU, Trondheim, Norway.

Gourlay, T. & Duncan, A. 2004. *Steady-state Towed Array Shape Calculation for a Circle Manoeuvre*. Centre for Marine Science and Technology, Curtin University of Technology, 468 (CS2004-01).

Hoerner, S.F., 1965. *Fluid-Dynamic Drag*. Published by the author, Brick Town, N.J., USA.

Patel, M.H. & Vaz, M.A. 1995. *Transient Behaviour of Towed Marine Cables in Two Dimensions*. Applied Ocean Research, Vol. 17, 143-153.

Perrault, D., Hackett, G. & Nahon, M. 1997. *Simulation and Active Control of Towed Undersea Vehicles*. IEEE Oceans ’97, Vol. 2, 1277-1282.

Sumer, B.M. & Fredsøe, J. 1999. *Hydrodynamics Around Cylindrical Structures*. World Scientific Publishing Pty. Ltd. Singapore, Singapore.